

## CHAPTER IV

### RESULT AND DISCUSSION

#### 4.1 The Study of Characteristics and Properties of Crude Oil

##### 4.1.1 Distillation

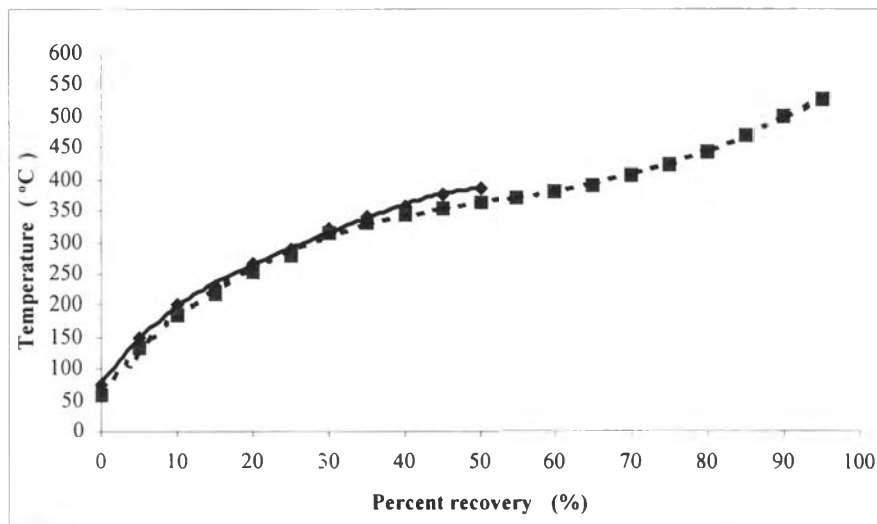
Both crude oils were distilled following the conventional method ASTM D86. Three tests each was conducted. They were also simulatedly distilled following the more sophisticated method ASTM D2887 employing the Sim-Dist GC. Carbon disulfide was used as solvent to dissolve 1 g of crude oil to 100 ml of carbon disulfide.

Table 4.1 shows the relationship of percent recovery and temperature as obtained from both ASTM D86 distillation and Sim-Dis GC of crude oils from Lankrabue and Uthong oil field. The three ASTM D86 distillation tests indicate fluctuating temperature read outs at various percent discovery, 400 °C at its maximum. For comparison, ASTM distillation data was plotted together with Sim-Dis GC data as shown in Figures 4.1, 4.2, and 4.3 for Lankrabue crude oil, and in Figures 4.4, 4.5, and 4.6 for U-Thong crude oil, respectively.

From these plots, it is evident that the distillation curves obtained from ASTM D86 of both Lankrabue and U-Thong crude oils were very close to those from Sim-Dis GC. Sim-Dist GC is therefore a very quick and reliable method to obtain a distillation curve of a crude oil. In addition, it was observed that the initial boiling point of Lankrabue crude oil is lower than that of U-Thong crude oil, i.e., 58.2 °C and 169.3 °C, respectively.

**Table 4.1** Percent recovery and temperature of Lankrabue and U-Thong crude oils

Percent recovery(%)	Temperature (°C)							
	Lankrabue crude oil				U-Thong crude oil			
	Test No.1.	Test No.2	Test No.3	Sim-Dis GC	Test No.1	Test No.2	Test No.3	Sim-Dis GC
0	75.5	65.0	60.5	58.2	166.0	167.0	171.5	169.3
5	150.0	142.0	140.0	133.2	226.0	225.0	232.5	227.1
10	202.0	190.0	195.5	185.6	261.0	256.0	263.0	260.1
15	231.5	221.5	223.0	218.4	289.5	285.5	287.5	285.5
20	265.0	260.5	264.0	252.4	327.5	315.5	317.5	318.6
25	288.5	280.0	290.5	278.6	342.5	335.5	334.5	332.6
30	320.0	311.5	316.5	314.0	352.5	343.5	341.5	342.2
35	341.5	329.5	334.0	329.8	360.5	349.5	352.0	349.4
40	356.5	345.0	352.0	343.1	368.5	358.0	359.0	356.4
45	377.5	360.5	364.0	353.5	374.5	365.0	367.0	362.1
50	386.0	372.0	375.5	362.1	383.0	373.0	374.0	369.0
55	-	385.5	388.0	372.7	391.0	383.5	383.0	376.9
60		395.0	398.0	382.0	-	395.5	-	384.7
65		-	-	392.8		-		396.3
70				407.2				410.7
75				424.1				427.9
80				445.6				450.7
85				471.0				478.1
90				502.9				509.9
95				528.4				529.7
FBP				540.3				540.4



**Figure 4.1** Relationship between temperature and percent recovery of test No.1 of Lankrabue crude oil a) dotted line and b) solid line showed the distillation curve obtained from Sim-Dis GC and from ASTM D86.

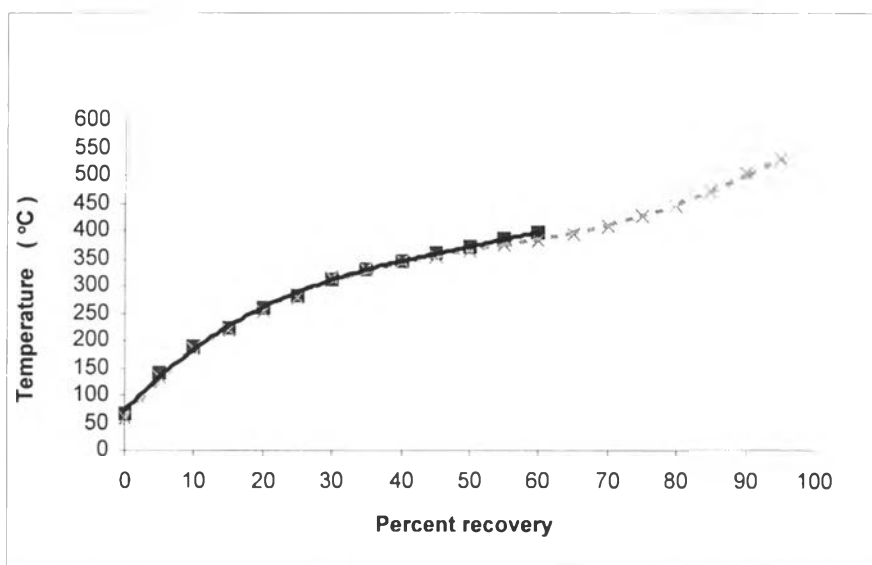


**Figure 4.2** Relationship between temperature and percent recovery of test No.2 of Lankrabue crude oil a) dotted line and b) solid line showed the distillation curve obtained from Sim-Dis GC and from ASTM D86.

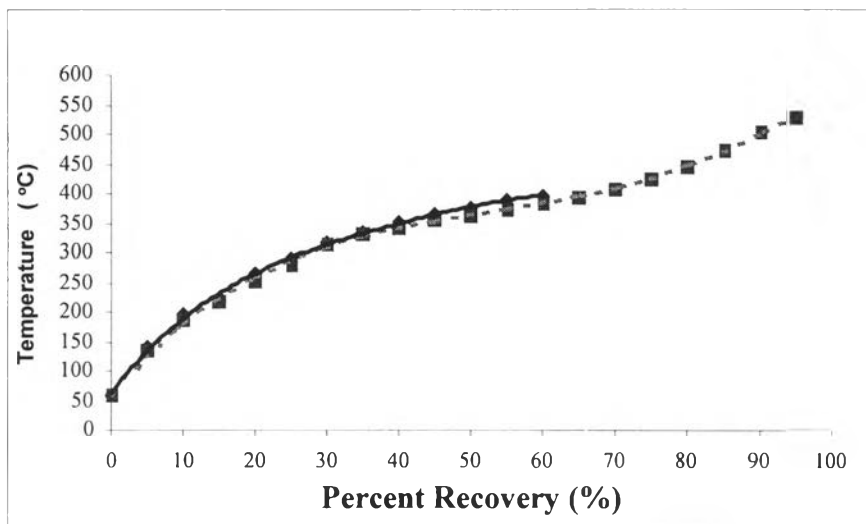


**Figure 4.3** Relationship between temperature and percent recovery of test No.3 of Lankrabue crude oil a) dotted line and b) solid line showed the distillation curve obtained from Sim-Dis GC and from ASTM D86.

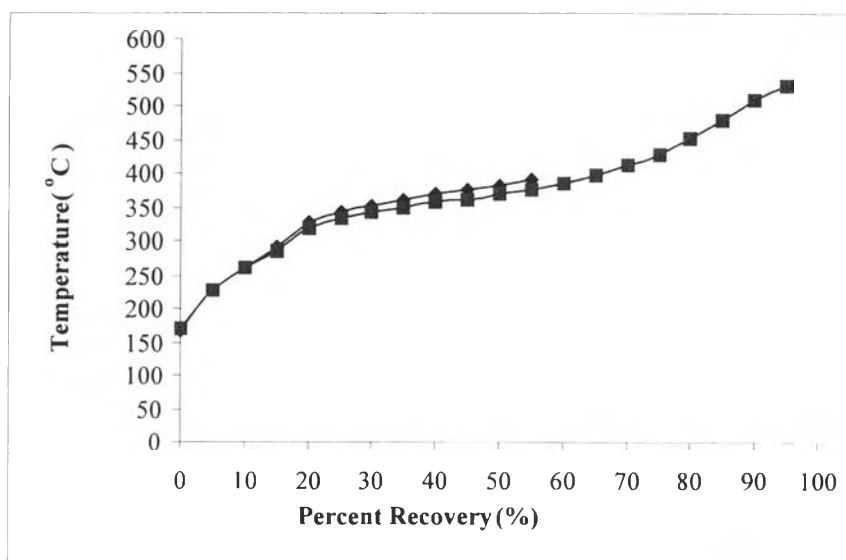


**Figure 4.4** Relationship between temperature and percent recovery of test No.1 of U-Thong crude oil a) dotted line and b) solid line showed the distillation curve obtained from Sim-Dis GC and from ASTM D86.

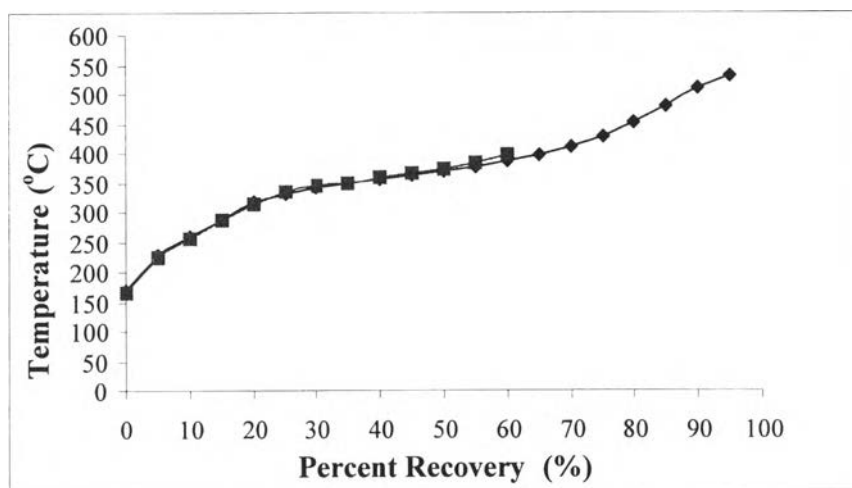


**Figure 4.5** Relationship between temperature and percent recovery of test No.2 of U-Thong crude oil a) dotted line and b) solid line showed the distillation curve obtained from Sim-Dis GC and from ASTM D86.

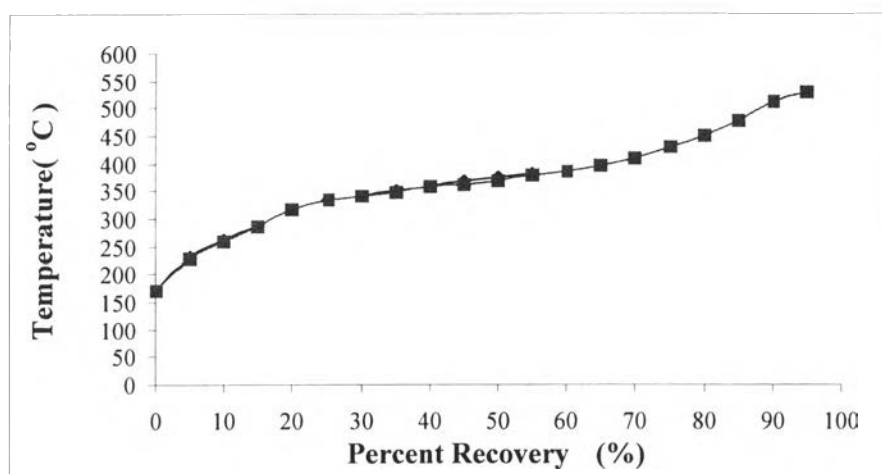


**Figure 4.6** Relationship between temperature and percent recovery of test No.2 of U-Thong crude oil a) dotted line and b) solid line showed the distillation curve obtained from Sim-Dis GC and from ASTM D86.

#### 4.1.2 Pour Point Testing

Table 4.2 shows pour point of both Lankrabue and U-Thong crude oil samples. From the data of pour point in both Tables, it indicates that pour points of both crude oil samples are different. U-Thong crude oil has the pour point lower than

that of the Lankrabue crude oil. When comparing with the composition of Sim-Dist GC chromatograms in Figures 4.7, and 4.8, it was found that the major hydrocarbon compositions of Lankrabue and U-Thong crude oil were in the range of C<sub>10</sub> to C<sub>24</sub> and C<sub>11</sub> to C<sub>24</sub>, respectively.

**Table 4.2** Pour point of Lankrabue and U-Thong crude oil

Sample	Pour Point ( °C)	
	Expected	Experiment
Lankrabue crude oil	40	38.0
	40	38.0
	40	37.0
	40	37.5
	Average	37.6
	Std. deviation	0.5
U-Thong crude oil	36	36.0
	36	35.5
	36	35.5
	36	35.5
	Average	35.6
	Std. deviation	0.25

#### 4.1.3 Density

Table 4.3 shows the densities of both both Lankrabue and U-Thong crude oil samples. This indicates that the density of Lankrabue crude oil was higher than that of U-Thong crude oil, despite the fact that Lankrabue crude oil has lower initial boiling point.

**Table 4.3** Density of Lankrabue at 41 °C and U-Thong Crude oil at 39 °C

Sample	Test No.	Density (g/cm <sup>3</sup> )
Lankrabue crude oil	1	0.879
	2	0.875
	3	0.880
	4	0.880
Average		<b>0.879</b>
U-Thong crude oil	1	0.855
	2	0.860
	3	0.850
	4	0.855
Average		<b>0.855</b>

## 4.2 Analysis

### 4.2.1 Identification of the Composition in Crude Oil

The composition of both Lankrabue and U-Thong crude oil samples that was analyzed by Sim-Dis GC was shown in Figures 4.7 and 4.8, respectively. The standard used is *n*-paraffins from C<sub>5</sub>-C<sub>44</sub> following ASTM D2887 and its chromatogram was shown in Appendix, Figure A-1. These Figures show that major *n*-paraffins of Lankrabue and U-Thong crude oils consist of carbon atom number in the C<sub>10</sub> – C<sub>24</sub> range and C<sub>11</sub>- C<sub>24</sub> range respectively. The quantification of hydrocarbon compositions of both crude oil samples was shown in Table 4.4 and the calculation is shown in Appendix B. This data indicates that the amount of *n*-paraffins of Lankrabue crude oil is higher than U-Thong crude oil. Moreover, it may be helped furthermore explain the effect of EVA and PMMA on macro-crystalline wax (*n*-parafins) for inhibiting wax deposition.

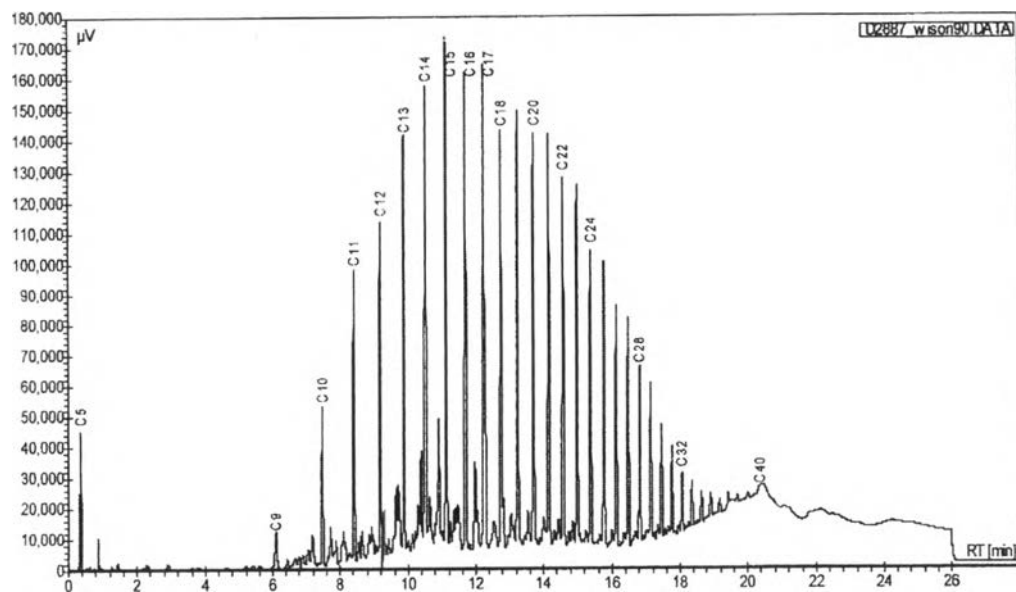


**Figure 4.7** Simulated Distillation Gas Chromatography chromatogram of Lankrabue crude oil.

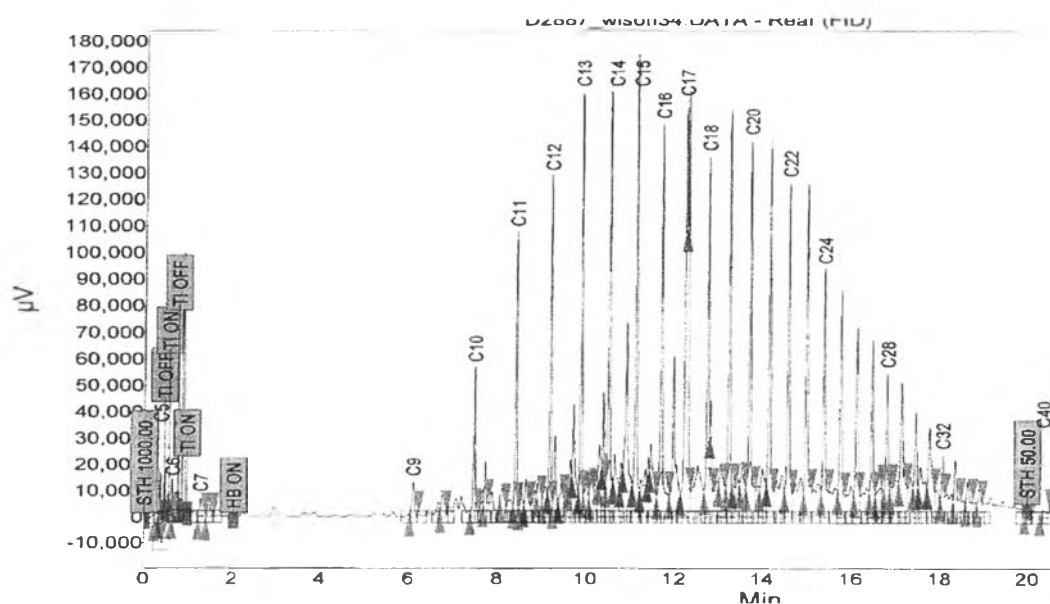


**Figure 4.8** Simulated Distillation Gas Chromatography chromatogram of U-Thong crude oil

**Table 4.4** Quantity of hydrocarbon composition of Lankrabue and U-Thong crude oil

Name	Formular	Weight Percent (%)	
		Lankrabue Crude oil	U-Thong Crude oil
Pentane	C <sub>5</sub> H <sub>12</sub>	0.1636	0.1680
Hexane	C <sub>6</sub> H <sub>14</sub>	-	0.0209
Heptane	C <sub>7</sub> H <sub>16</sub>	-	0.0261
Octane	C <sub>8</sub> H <sub>18</sub>	-	-
Nonane	C <sub>9</sub> H <sub>20</sub>	0.0797	0.0824
Decane	C <sub>10</sub> H <sub>22</sub>	0.2334	0.2502
Undecane	C <sub>11</sub> H <sub>24</sub>	0.3670	0.3930
Dodecane	C <sub>12</sub> H <sub>26</sub>	0.4753	0.5179
Tridecane	C <sub>13</sub> H <sub>28</sub>	0.6293	0.6787
Tetradecane	C <sub>14</sub> H <sub>30</sub>	0.8448	0.8983
Pentadecane	C <sub>15</sub> H <sub>32</sub>	0.8988	0.9305
Hexadecane	C <sub>16</sub> H <sub>34</sub>	0.8548	0.8979
Heptadecane	C <sub>17</sub> H <sub>36</sub>	1.3707	0.9885
Octadecane	C <sub>18</sub> H <sub>38</sub>	1.0176	0.8123
Eicosane	C <sub>20</sub> H <sub>42</sub>	1.0637	1.1057
Docosane	C <sub>22</sub> H <sub>44</sub>	0.9535	1.0185
Tetracosane	C <sub>24</sub> H <sub>50</sub>	1.1708	1.1843
Octacosane	C <sub>28</sub> H <sub>58</sub>	0.9796	0.8972
Dotriacontane	C <sub>32</sub> H <sub>66</sub>	0.6117	0.4940
Hexatriacontane	C <sub>36</sub> H <sub>74</sub>	-	-
Tetracontane	C <sub>40</sub> H <sub>82</sub>	1.1601	0.2032
Tetratetracontane	C <sub>44</sub> H <sub>90</sub>	-	-
Total		12.8746	11.5677

## 4.2.2 Analyzing the Separated Fraction of Crude Oil

### 4.2.2.1 Using Sim-Dis GC

The micro- and macro-crystalline wax of Lankrabue and U-Thong crude oil as obtained from both Nguyen's method and modified from Nguyen's method were shown in Figures 4.9, 4.10, 4.11, 4.12, 4.13, 4.14, 4.15, and 4.16, respectively. From the chromatogram, if GC chromatograms of micro-crystalline wax (*iso*- and *cyclo*-paraffins) of both crude oils as obtained from both methods were compared with those of macro-crystalline wax e.g. Figures 4.9 and 4.13, it is found that the peaks of hydrocarbons in micro-crystalline wax shift from the standard peak of *n*-paraffins. This is the preliminary result and it is evident that wax fractions of both crude oils as obtained from both methods are different. This was further confirmed by FTIR analyses.

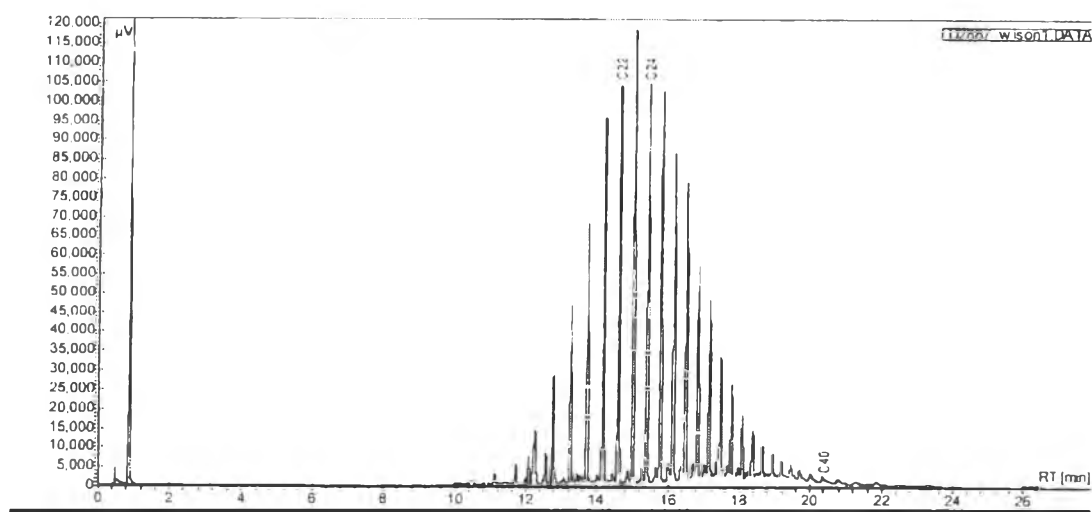


**Figure 4.9** GC chromatogram of micro-crystalline wax of Lankrabue crude oil as obtained from Nguyen's method.

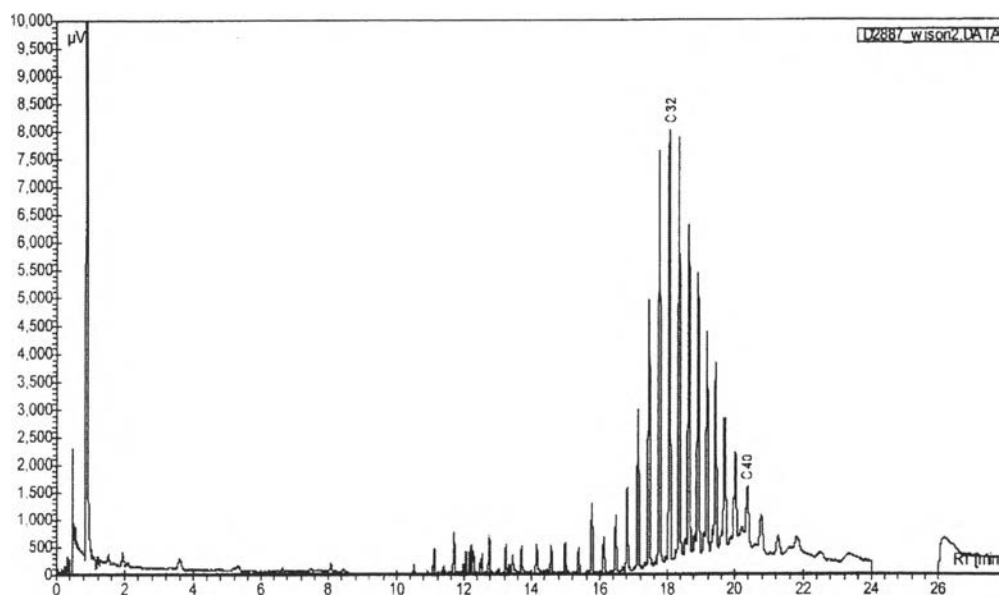


**Figure 4.10** GC chromatogram of micro-crystalline wax of Lankrabue crude oil as obtained from modified method.

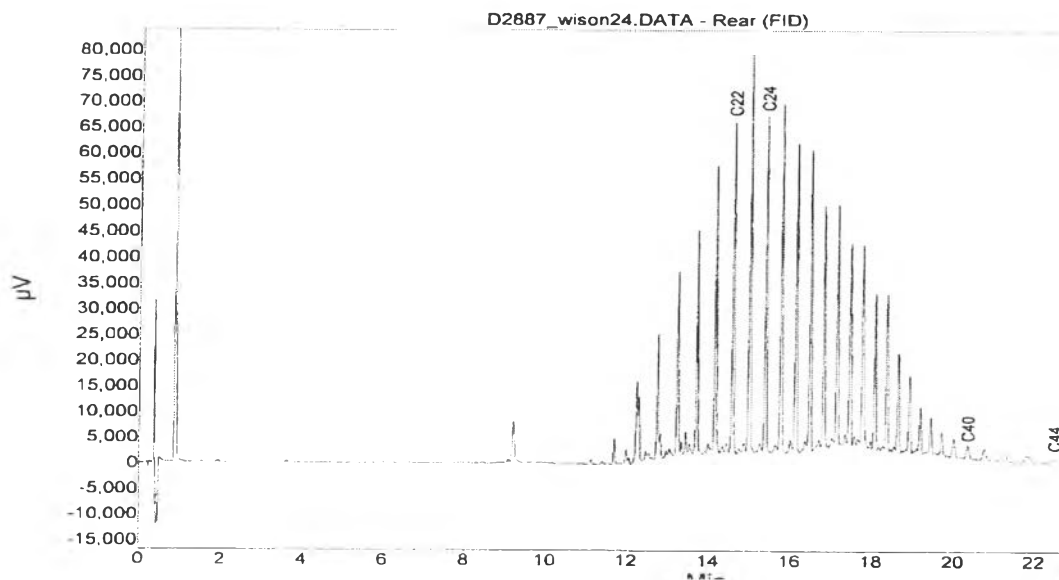


**Figure 4.11** GC chromatogram of micro-crystalline wax of U-Thong crude oil as obtained from Nguyen's method.

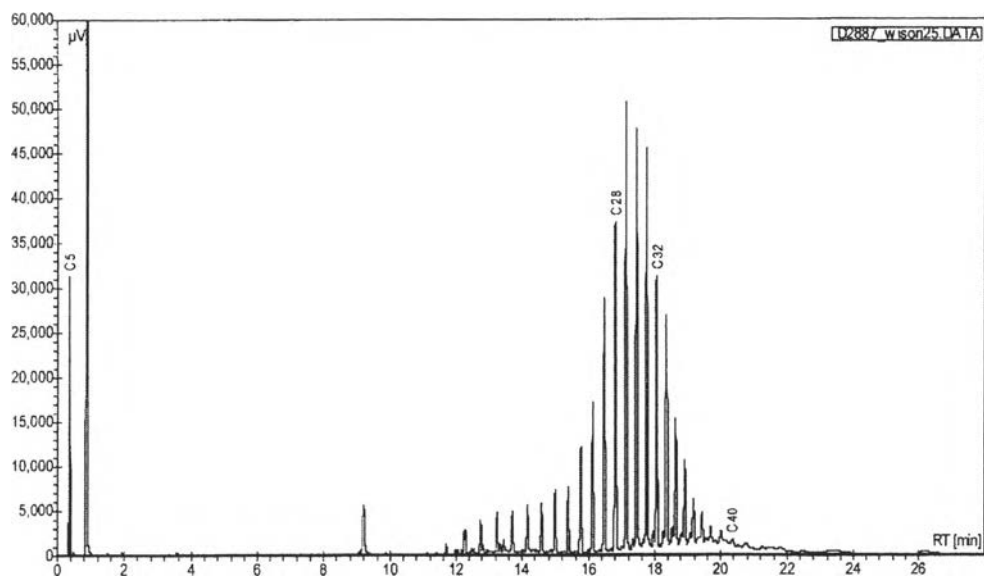


**Figure 4.12** GC chromatogram of micro-crystalline wax of U-Thong crude oil as obtained from modified method.

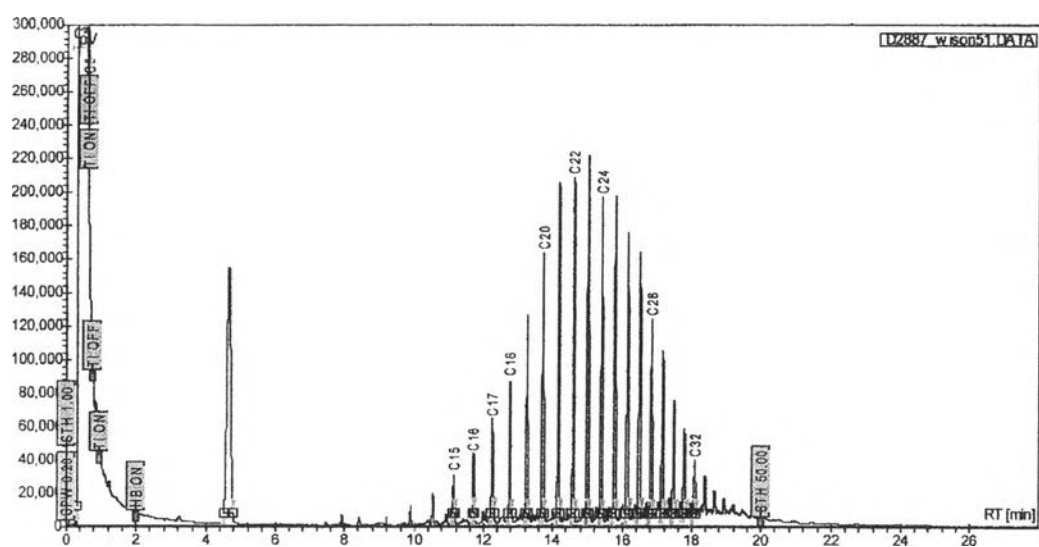


**Figure 4.13** GC chromatogram of macro-crystalline wax of Lankrabue crude oil as obtained from Nguyen's method.

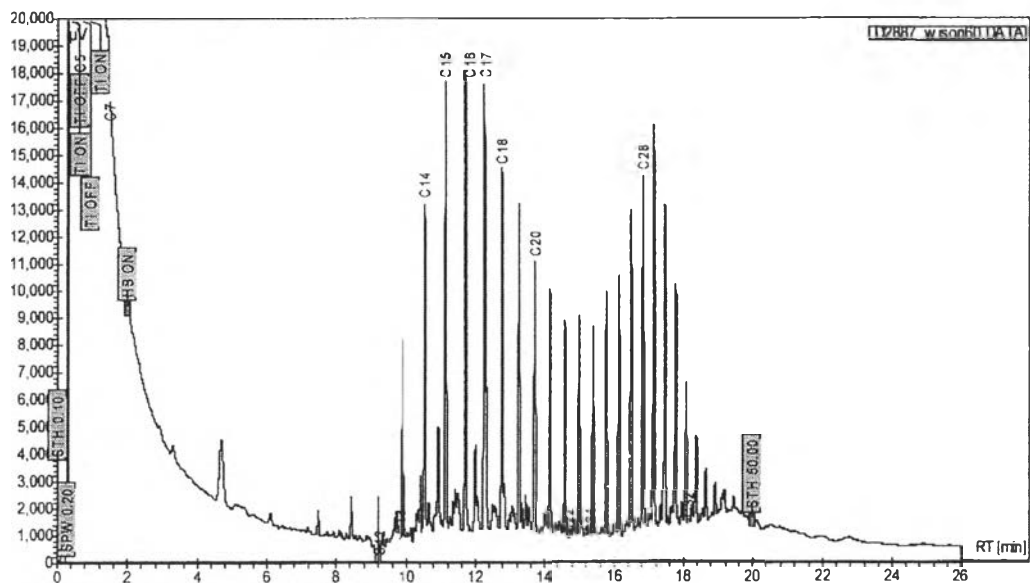


**Figure 4.14** GC chromatogram of macro-crystalline wax of Lankrabue crude oil as obtained from modified method.

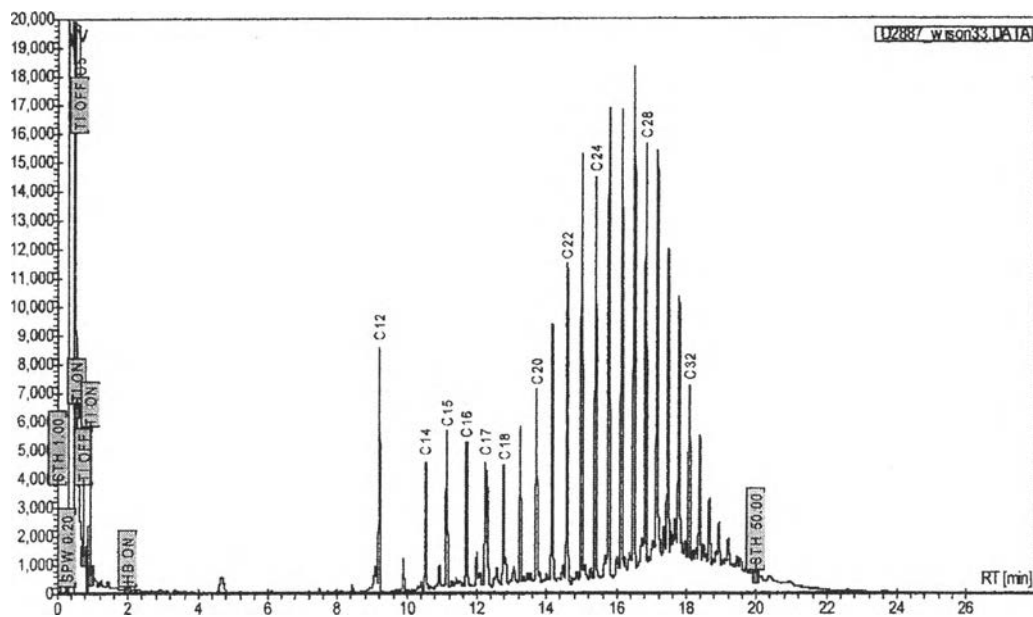


**Figure 4.15** GC chromatogram of macro-crystalline wax of U-Thong crude oil as obtained from Nguyen's method.

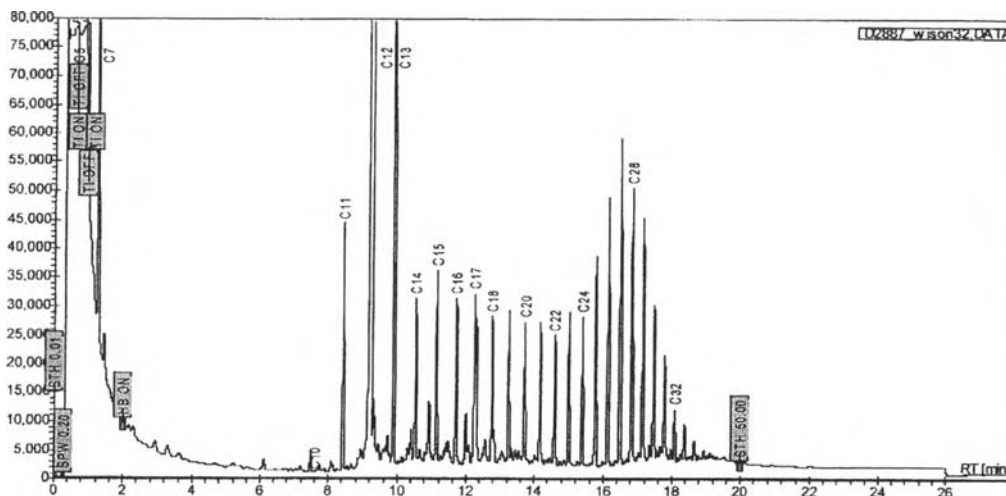


**Figure 4.16** GC chromatogram of macro-crystalline wax of U-Thong crude oil as obtained from modified method.

#### 4.2.2.2 Using FTIR

The infrared (IR) spectra of asphaltene fraction of both crude oil methods were shown in Figure of both crude oil as obtained from both methods were shown in Figure 4.17, 4.18, and micro- and macro-crystalline wax fraction were shown in Figure 4.20, 4.21, 4.22, 4.23, 4.25, 4.26, 4.27, 4.28 and 4.29. Also, the IR spectrum of reference of micro-crystalline wax as obtained from [www.fao.org](http://www.fao.org) and of macro-crystalline wax as obtained from dodecane ( $C_{12}H_{26}$ ) were shown in Figure 4.19 and 4.24, respectively.

One well known fact is that the major components in crude oil consist of asphaltenes, resins, and saturates (micro- and macro-crystalline wax). Therefore, the obtained micro- and macro-crystalline wax fractions must be confirmed that they are free from asphaltenes and resins by considering the characteristic peak of asphaltenes and resins which appear at  $3600-3300\text{ cm}^{-1}$  for OH and NH group, and at  $2200-1667\text{ cm}^{-1}$  for overtone and combination bands. From the IR spectra of both waxes fraction, it is evident that they are free from asphaltene and resin because those characteristic peaks of asphaltenes and resins did not appear, although very strong bands corresponding to methyl group stretching vibrations are observed at  $3000-2800\text{ cm}^{-1}$  for asphaltenes, resin and both wax crystal.

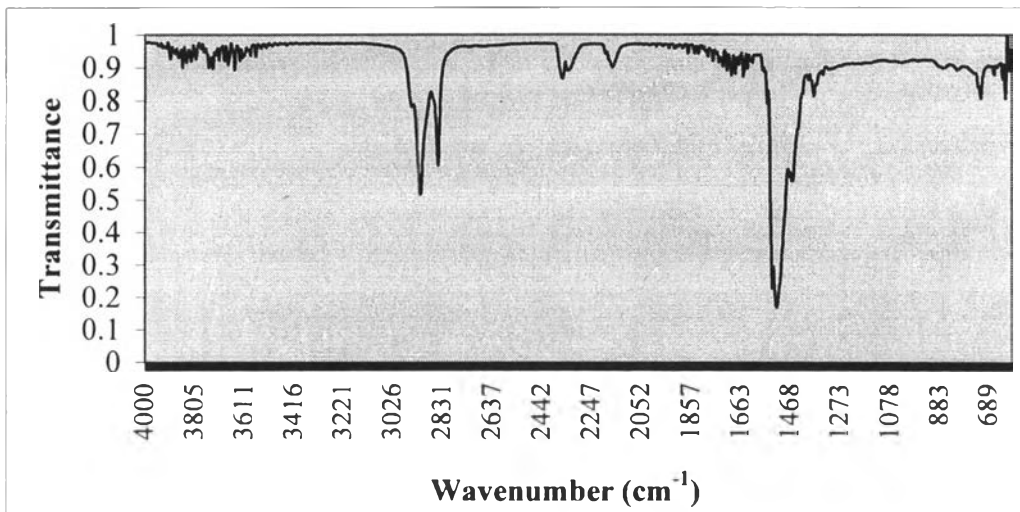


**Figure 4.17** IR spectrum of asphaltene fraction of Lankrabue crude oil.

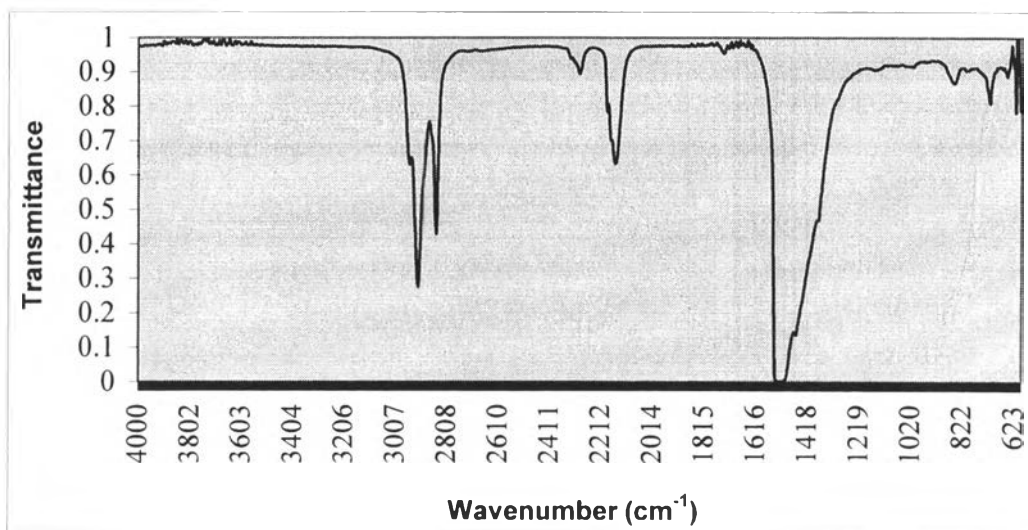


**Figure 4.18** IR spectrum of asphaltene fraction of U-Thong crude oil.

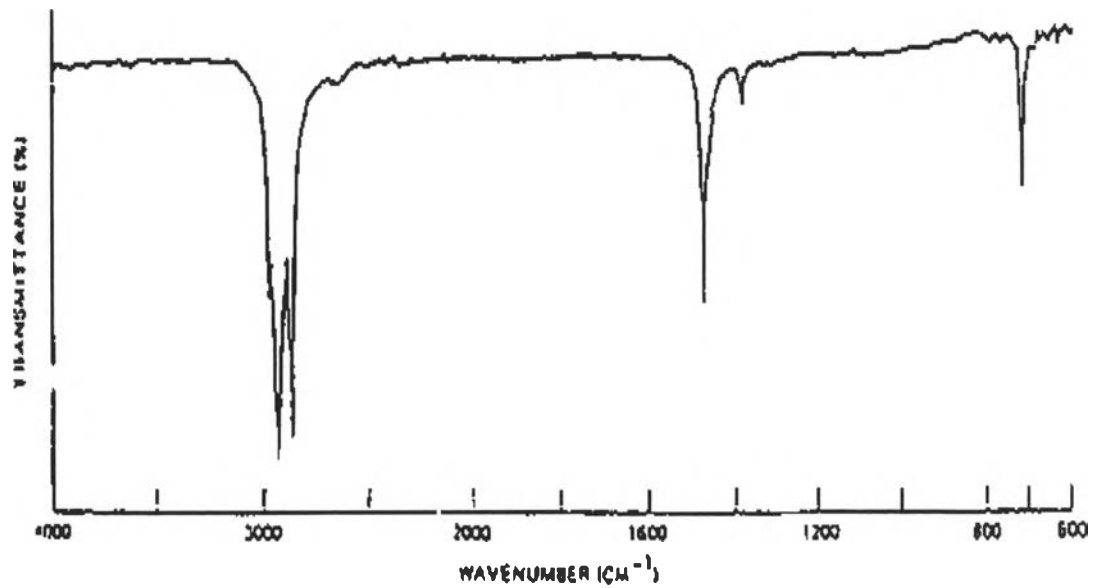


**Figure 4.19** IR spectrum of reference of micro-crystalline wax as obtained from [www.fao.org](http://www.fao.org).

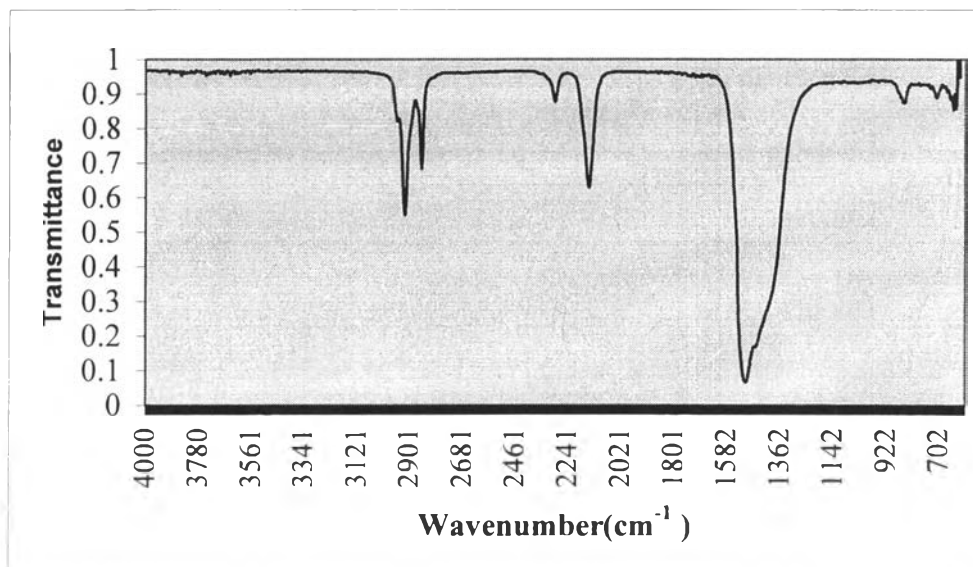


**Figure 4.20** IR spectrum of micro-crystalline wax of Lankrabue crude oil as obtained from Nguyen's method.

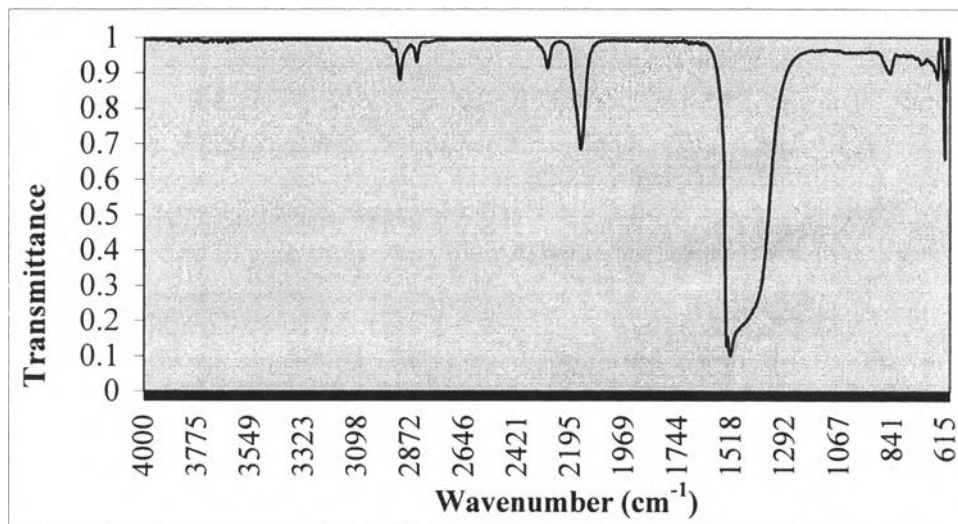


**Figure 4.21** IR spectrum of micro-crystalline wax of Lankrabue crude oil as obtained from modified method.

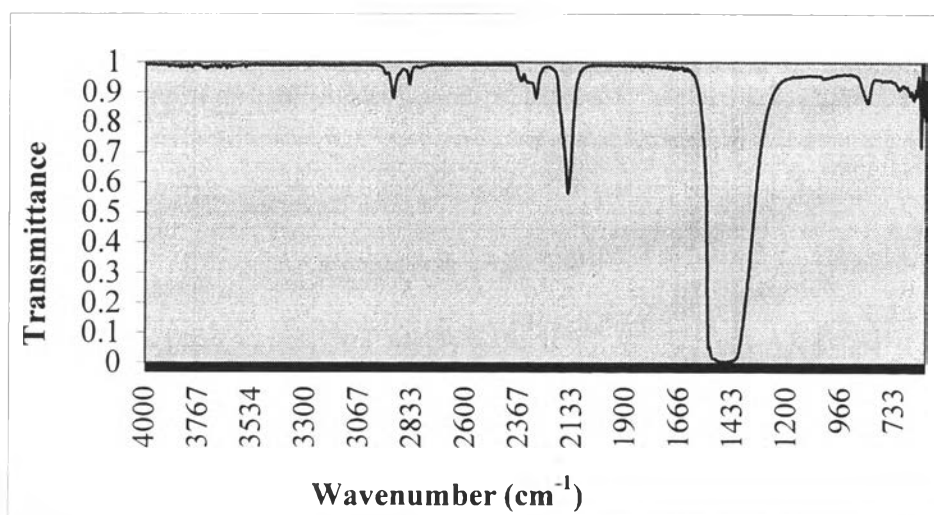


**Figure 4.22** IR spectrum of micro-crystalline wax of U-Thong crude oil as obtained from Nguyen's method.

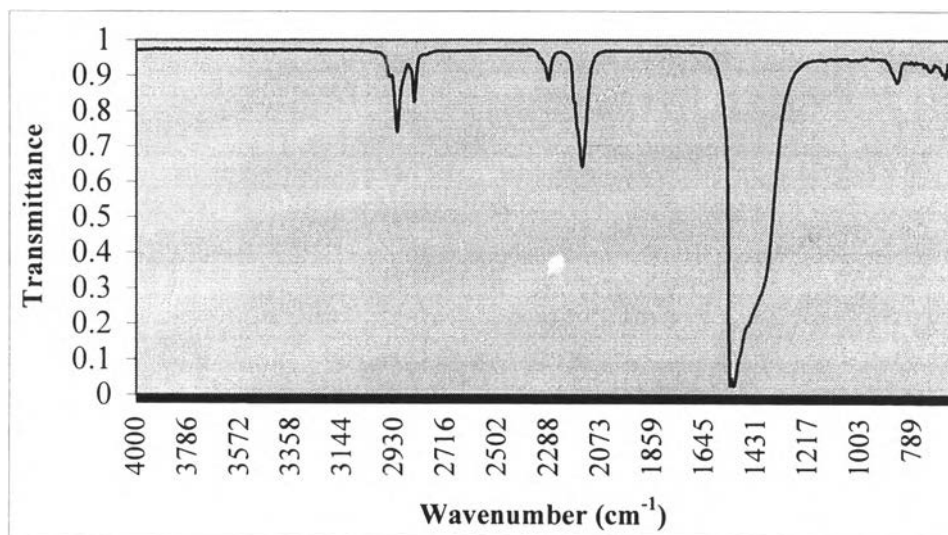


**Figure 4.23** IR spectrum of micro-crystalline wax of U-Thong crude oil as obtained from modified method.

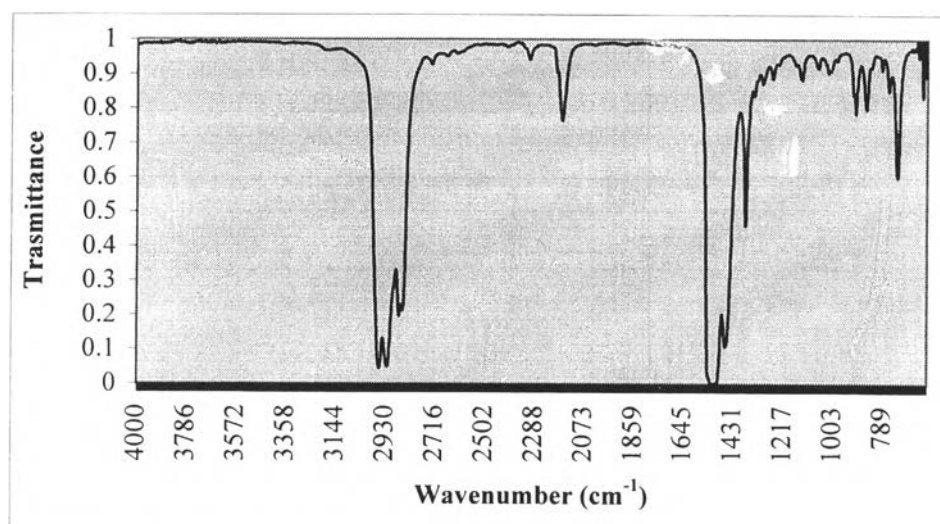


**Figure 4.24** IR spectrum of reference of macro-crystalline wax as obtained from dodecane (C<sub>12</sub>H<sub>26</sub>).

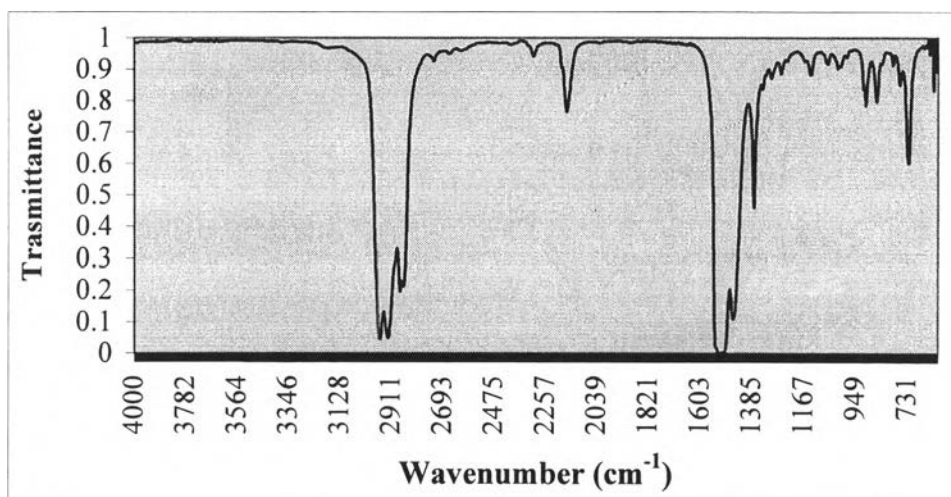


**Figure 4.25** IR spectrum of macro-crystalline wax of Lankrabue crude oil as obtained from Nguyen's method.

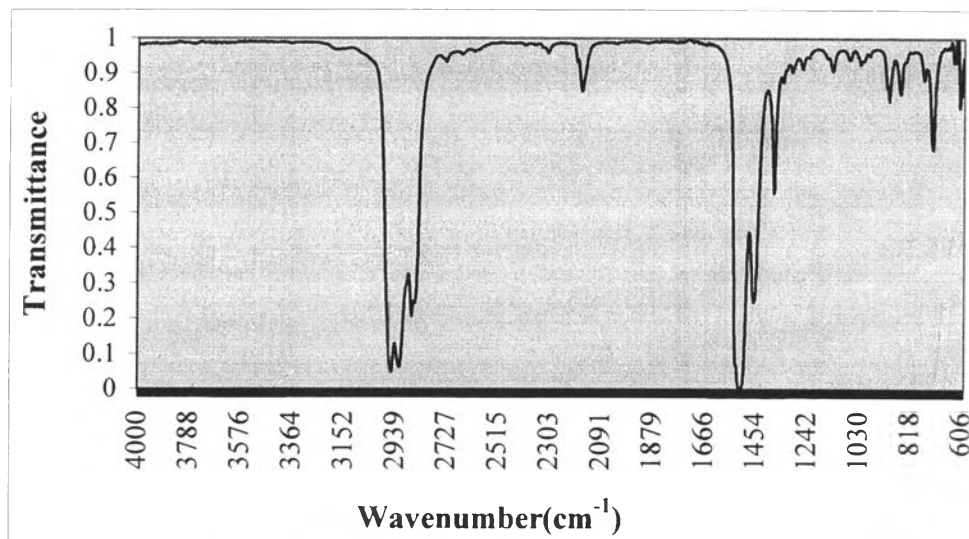


**Figure 4.26** IR spectrum of macro-crystalline wax of Lankrabue crude oil as obtained from modified method.

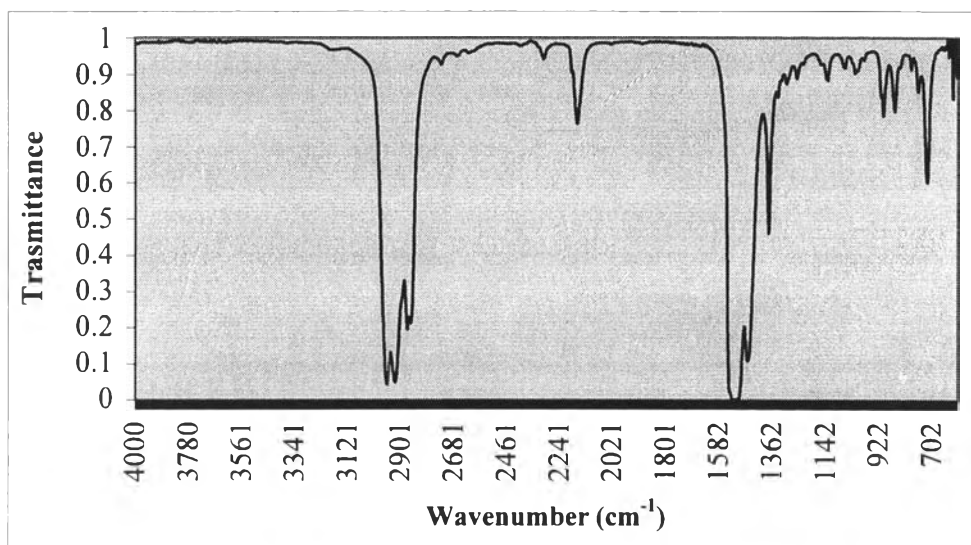


**Figure 4.27** IR spectrum of macro-crystalline wax of U-Thong crude oil as obtained from Nguyen's method.

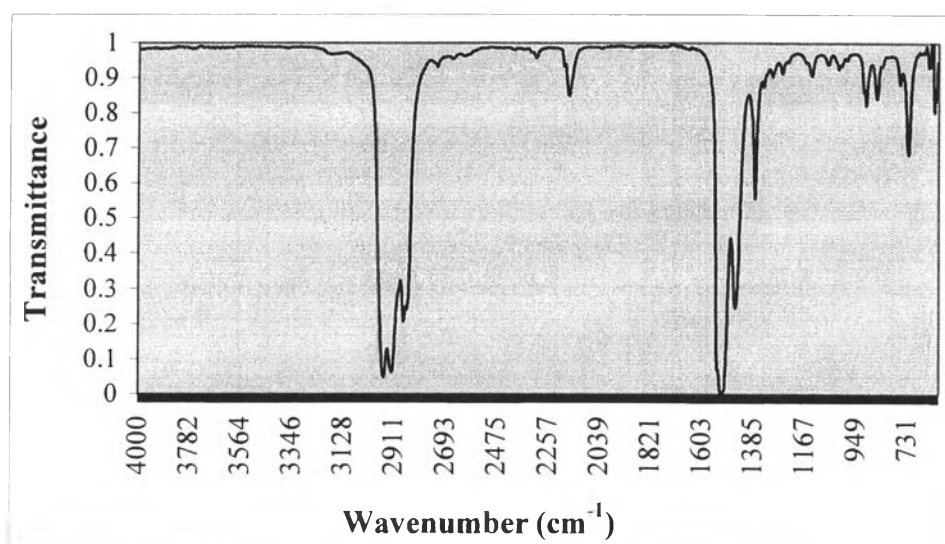


**Figure 4.28** IR spectrum of macro-crystalline wax of U-Thong crude oil as obtained from modified method.

The IR spectra of micro-crystalline wax was identified by comparing with the reference spectra. The characteristic peaks of micro-crystalline wax appear at 1450 cm<sup>-1</sup> for alicyclic -CH<sub>2</sub>- scissor and 1395 cm<sup>-1</sup> for symmetric

CH<sub>3</sub> bending (*iso*- and *tert*- alkyl). When the spectra of all micro-crystalline wax fractions were compared with the reference, it is found that they compared very well because, although, before micro-crystalline wax fraction were analyzed by FTIR, they were dissolved in CS<sub>2</sub> which has characteristic peak at 2195 – 2400 cm<sup>-1</sup> and 1450 cm<sup>-1</sup> bands for C-S bond, their spectra are still very similar with that of reference. So with these comparisons, they can be confirmed that after the wax fractions were separated by *n*-pentane with both methods, similarly, all precipitates of both crude oils are true micro-crystalline wax fractions.

Similarly, the macro-crystalline wax fractions that are *n*-paraffins were compared with the reference. The characteristic peaks of macro-crystalline wax appear at 1380 – 1375 cm<sup>-1</sup> for CH<sub>3</sub> symmetric and 1470-1460 cm<sup>-1</sup> for aliphatic CH<sub>2</sub> scissor. The IR spectra of all macro-crystalline wax fractions were compared with the reference, and they compared very well. Therefore, it can be concluded that the wax fractions that are solutes in *n*-pentane are true macro-crystalline wax.

From the FTIR findings, one can conclude that both separation methods can separate the micro-crystalline wax fraction from the macro-crystalline wax fraction very effectively, and that the modified method is less time-consuming than Nguyen's method.

#### 4.2.2.3 Quantity of separated fraction

The amount of waxes (micro- and macro-crystalline wax) as obtained from both Nguyen's method and modified from Nguyen's method is shown in Table 4.5. The results indicate that the amount of waxes fraction as obtained from Nguyen's method is higher than that of obtained from modified Nguyen's method.

If the procedure of both separation methods is considered, the main difference lies in the part of removing asphaltenes and resins fraction from saturates fraction (micro- and macro-crystalline wax). In Nguyen's method, asphaltenes and resins were removed by using *p*-xylene. But, in the modified method, they were removed by using *n*-heptane. The explanation is in the fact that the polarity of *p*-xylene is higher than *n*-heptane therefore the waxes as obtained from the modified method is lower than that of obtained from Nguyen's method.

When combining both wax fractions obtained from both methods and comparing them with the total wax (micro- and macro-crystalline wax) as obtained from standard UOP46-64 method, it is found that they are lower, as shown in Table 4.5. One possible reason is the different solvent used in removing other components from waxes. The UOP46-64 standard uses mixture of acetone and petroleum ether which has higher polarity than the neat acetone which is used in the separation by modified and Nguyen's method.

**Table 4.5** Percent content of waxes fraction as obtained from Nguyen's, modified and standard UOP46-64 method

Type of sample	Method	Percent content (%)		
		micro-crystalline wax	macro-crystalline wax	Total wax
Lankrabue crude oil	Nguyen's	4.99	17.94	22.93
	Modified	5.17	14.68	19.84
	Standard UOP 46-64	-		24.32
U-Thong crude oil	Nguyen's	6.50	14.43	20.93
	Modified	7.65	12.10	19.75
	Standard UOP 46-64	-		21.20

#### 4.2.3 Wax Appearance Temperature (WAT) and Wax Dissolution Temperature (WDT)

From the result obtained from DSC equipment, one can deduce that WAT of Lankrabue crude oil is about 42 °C and is higher than WAT of U-Thong crude oil that is about 37 °C. Also, the WDT appeared at 52 °C and 49 °C for Lankrabue and U-Thong crude oil respectively. Their thermograms were shown in Figures 4.29, 4.30, 4.31, and 4.32, respectively.

In the thermogram, it becomes evident that WDT is always higher than WAT. The difference between WAT and WDT might be due to undercooling and overheating that result in non-equilibrium conditions during fast temperature scanning (Elshakawy *et al.*, 2000). Hansen *et al.* (1991) recommended that this problem can be avoided by using very low scanning temperature. However, the low temperature scanning ( 2-3 °C/min ) would reduce the DSC sensitivity as the DSC signal is the time derivative of heat flow. Another reason for the difference between WAT and WDT that should not be overlooked is due to the difficulty in defining appropriate processing baseline and the bad signal to noise ratios and leading/ending transients of some of the thermograms that made it very difficult to determine the processing temperature limits.

In addition, the small peak at 45 to 48 °C in thermogram of cooling curve of Lankrabue crude oil resembles what was recently observed in waxes with a high ratio of macrocrystalline to microcrystalline wax (Faust *et al.*, 1978). Hence, it might be concluded that these peaks are associated with the thermal transitions (liquid to solid and vice versa) of macrocrystalline wax consisting of mainly *n*-paraffins, while the remaining shallow but broader peak of the thermogram is due to the more complicated thermal transitions of the crystalline-amorphous wax phases including solid-solid transitions, e.g., orthorhombic-hexagonal transitions as Turner (1971) described for the intermediate *n*-paraffin range C<sub>20</sub>-C<sub>40</sub>.

From the thermograms, the wax precipitation enthalpy ( $\Delta H_{\text{wat}}$ ) of Lankrabue and U-Thong crude oil could be calculated and is found to be 44.57 j/g and 33.71 j/g, respectively, and the wax dissolution enthalpy ( $\Delta H_{\text{wdt}}$ ) of Lankrabue and U-Thong is found to be 50.02 j/g and 39.77 j/g, respectively. Similar to the WAT and WDT,  $\Delta H_{\text{wdt}}$  are greater than  $\Delta H_{\text{wat}}$ .

The enthalpy obtained from the energy released during cooling is proportional to the area enclosed by the exotherm and the processing baseline as shown in Figures 4.29 and 4.31. This area can be defined as only wax precipitation since other precipitates such as asphaltene, resin etc., are not effected by thermal application as measured by DSC. Moreover, cooling crude oil in a moderate temperature range would not lead to asphaltene and resin precipitation. This last

phenomenon is more connected to changes of either crude composition or to pressure variations.

The difference in enthalpy of any crude oils probably reflected their varying composition and content of wax precipitate which it has been observed by Glavaniri *et al.* (1973) that the transition enthalpy was in linear relationship with *n*-paraffin content. In addition to the enthalpy involved, the liquid-solid transitions as spike peaks were supposed to originate from the initial crystallization of a limited range of *n*-paraffins at the beginning of the cooling process, and the broad exotherms probably also included the enthalpy involved in intra-crystal solid-solid transitions (Turner, 1971).

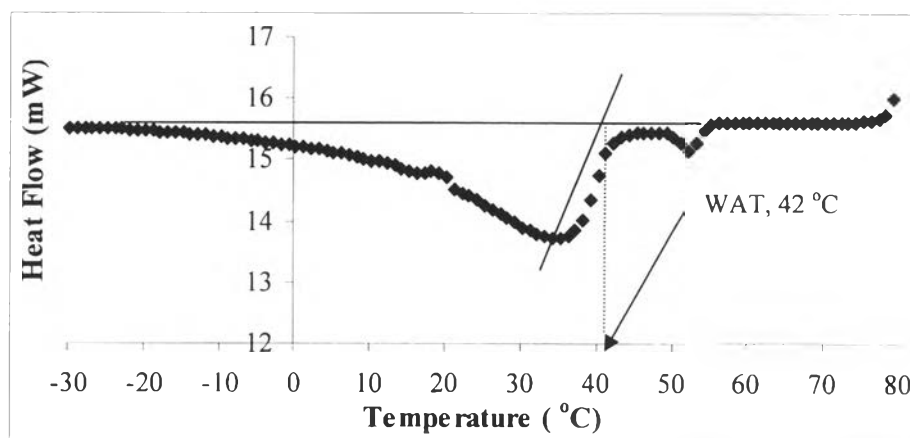


**Figure 4.29** DSC thermogram obtained by cooling from 80 °C to -30 °C of Lankrabue crude oil.

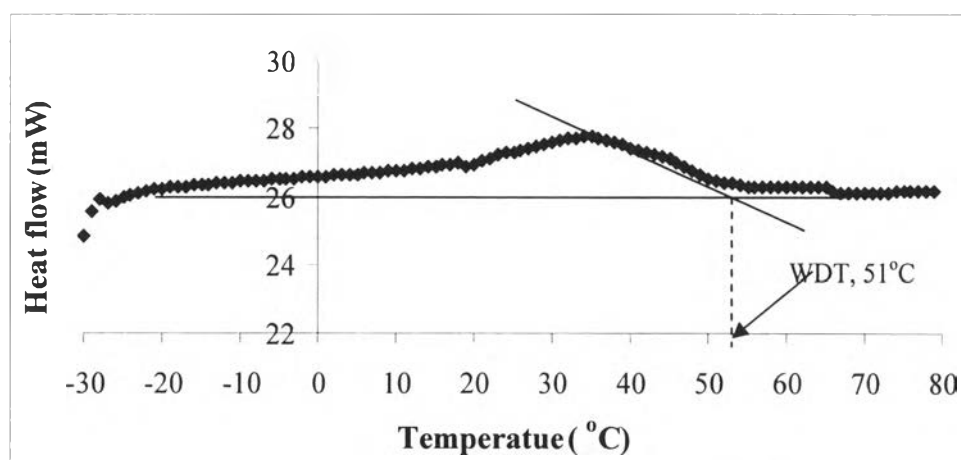


**Figure 4.30** DSC thermogram obtained by heating from  $-30\text{ }^{\circ}\text{C}$  to  $80\text{ }^{\circ}\text{C}$  of Lankrabue crude oil.

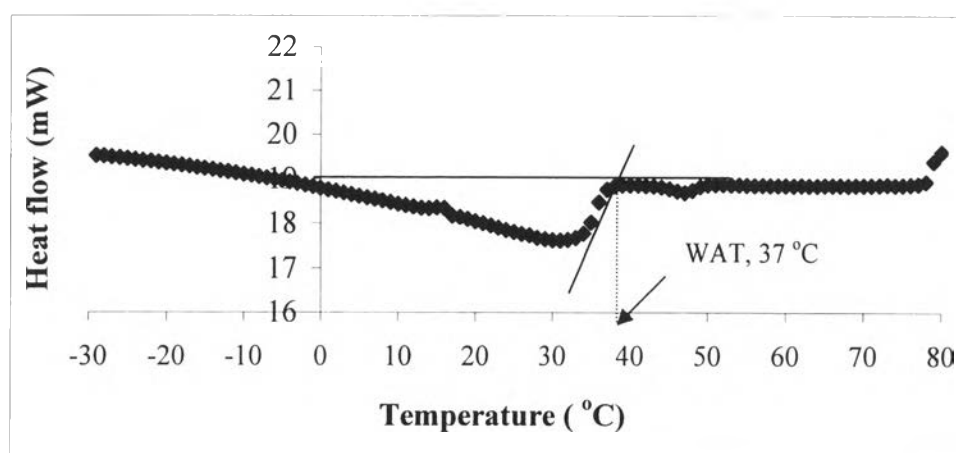


**Figure 4.31** DSC thermogram obtained by cooling from  $80\text{ }^{\circ}\text{C}$  to  $-30\text{ }^{\circ}\text{C}$  of U-Thong crude oil.

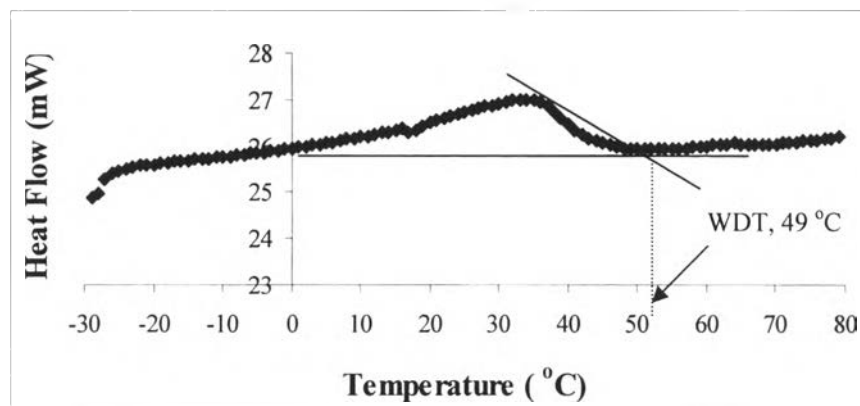


**Figure 4.32** DSC thermogram obtained by heating from -30 to 80 °C of U-Thong crude oil.

### 4.3 Quantification of the Amount of Wax

#### 4.3.1 Wax Content

The raw data of wax content of crude oil samples that was determined following the method in item 3.4.1 is shown in Appendix A, Table A-1. As shown in the Table A-1, it is found that the total wax content of Lankrabue crude oil is higher than U-Thong crude oil at 24.32 and 21.20%, respectively.

#### 4.3.2 Relationship between Percent Wax Deposition and Temperature

The relationship between percent wax deposition and temperature is shown in Figures 4.33 and 4.34 for Lankrabue and U-Thong crude oil, respectively. From these figures, it is evident that the amount of wax deposition of Lankrabue crude oil at any temperature is higher than that of U-Thong crude oil. These results correlate well with the results from wax content.

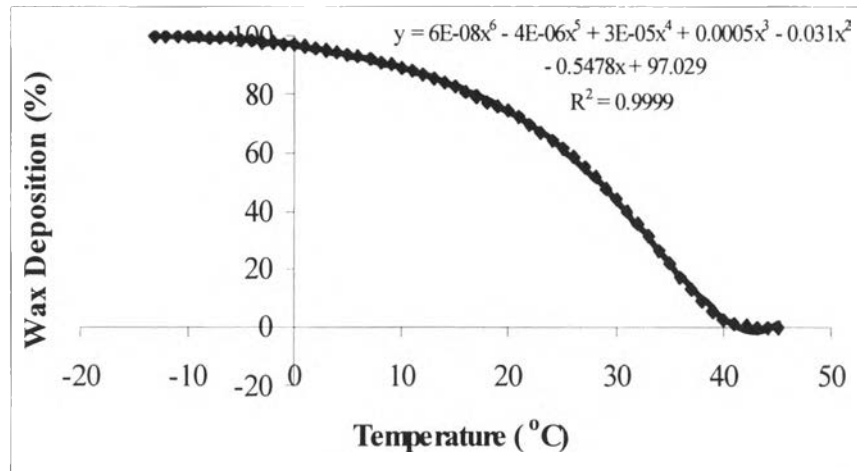


**Figure 4.33** Relationship between percent wax deposition and temperature of Lankrabue crude oil.

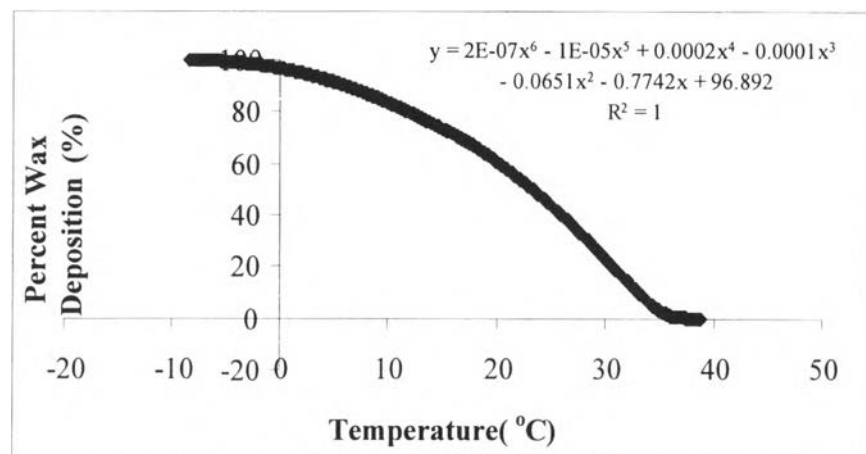


**Figure 4.34** Relationship between percent wax deposition and temperature of U-Thong crude oil.

#### **4.4 Investigation of the Chemical Method to Solve Wax Deposition Problem**

Pour points of both Lankrabue and U-Thong crude oils as added by EVA and PMMA at any concentration are shown in Tables 4.5, 4.6, 4.7, and 4.8, respectively, indicates that the maximum reduction of pour point of treated Lankrabue crude oil was obtained when it is treated by PMMA, VH grade, at 1000 ppm, and the maximum reduction of pour point of treated U-Thong crude oil was obtained when it is treated by EVA containing 25% content of VA, at 200 ppm. The comparison purpose, barcharts of pour point of both treated crude oils by EVA and PMMA were plotted as shown in Figures 4.35, 4.36, 4.37, and 4.38, respectively.

**Table 4.5** Pour Point of treated Lankrabue crude oil by EVA

Percent Content of VA in EVA	Concentration (PPM, wt/wt)	Pour Point (°C)				
		Test No.1	Test No.2	Test No.3	Average	Standard deviation
18	100	36.5	36.0	36.5	36.3	0.3
	200	35.0	35.0	35.0	35.0	0.0
	400	35.0	35.0	35.5	35.2	0.3
	600	34.0	34.5	34.0	34.2	0.3
	800	36.5	36.0	36.5	36.3	0.3
	1000	38.0	38.0	38.5	38.2	0.3
25	100	34.0	34.5	34.0	34.2	0.3
	200	32.5	32.5	32.5	32.5	0.0
	400	31.0	31.5	31.0	31.2	0.3
	600	30.0	30.0	30.0	30.0	0.0
	800	27.0	26.5	26.5	26.7	0.3
	1000	32.5	32.0	32.5	32.3	0.3
33	100	34.0	34.0	34.0	34.0	0.0
	200	35.0	35.0	34.5	34.8	0.3
	400	33.0	32.5	32.5	32.7	0.3
	600	32.5	31.5	31.0	31.7	0.8
	800	35.5	36.0	35.5	35.7	0.3
	1000	36.5	37.0	37.0	36.8	0.3
40	100	38.0	38.5	38.0	38.2	0.3
	200	37.0	37.5	37.0	37.2	0.3
	400	36.5	36.0	36.5	36.3	0.3
	600	37.0	37.5	38.0	37.5	0.5
	800	38.0	38.5	38.0	38.2	0.3
	1000	39.0	39.0	39.0	39.0	0.0

**Table 4.6** Pour Point of treated U-Thong crude oil by EVA

Percent Content of VA in EVA	Concentration (PPM, wt/wt)	Pour Point ( °C)				
		Test No.1	Test No.2	Test No.3	Average	Standard deviation
18	100	33.0	33.5	33.0	33.2	0.3
	200	30.0	30.0	30.5	30.2	0.3
	400	28.0	28.5	28.0	28.2	0.3
	600	26.0	26.5	26.0	26.2	0.3
	800	28.0	28.5	28.5	28.3	0.3
	1000	29.0	29.0	29.5	29.2	0.3
25	100	27.0	26.5	26.5	26.7	0.3
	200	20.0	20.0	20.0	20.0	0.0
	400	22.0	22.5	22.0	22.2	0.3
	600	25.0	25.5	25.0	25.2	0.3
	800	26.0	26.0	26.0	26.0	0.0
	1000	34.0	33.5	34.0	33.8	0.3
33	100	33.0	33.5	33.0	33.2	0.3
	200	34.0	34.0	34.0	34.0	0.0
	400	25.0	24.5	25.0	24.8	0.3
	600	30.5	31.0	31.0	30.8	0.3
	800	33.0	33.0	33.5	33.2	0.3
	1000	31.0	31.0	31.0	31.0	0.0
40	100	29.0	29.0	29.5	29.2	0.3
	200	32.0	32.5	32.0	32.2	0.3
	400	27.0	27.5	27.0	27.2	0.3
	600	32.0	32.0	32.0	32.0	0.0
	800	33.0	33.5	33.0	33.2	0.3
	1000	34.0	34.5	34.0	34.2	0.3

**Table 4.7** Pour Point of treated Lankrabue crude oil by PMMA

Concentration of PMMA	Pour Point ( °C)									
	VH					MD				
	Test No.1	Test No.2	Test No.3	Avg.	Stdev.	Test No.1	Test No.2	Test No.3	Avg.	Stdev.
100	26.0	26.5	26.0	26.2	0.3	34.0	34.0	34.5	34.2	0.3
200	28.0	28.5	28.0	28.2	0.3	36.0	36.5	36.0	36.2	0.3
400	28.0	28.0	28.0	28.0	0.0	34.0	34.0	34.0	34.0	0.0
600	30.0	30.5	30.5	30.3	0.3	34.0	34.0	34.0	34.0	0.0
800	30.0	30.0	30.0	30.0	0.0	38.0	38.0	38.0	37.5	0.0
1000	24.0	24.0	24.5	24.2	0.3	33.0	32.5	33.0	32.8	0.3

**Table 4.8** Pour Point of treated U-Thong crude oil by PMMA

Concentration of PMMA	Pour Point ( °C)									
	VH					MD				
	Test No.1	Test No.2	Test No.3	Avg.	Stdev.	Test No.1	Test No.2	Test No.3	Avg.	Stdev.
100	36.0	36.0	36.0	36.0	0.0	32.0	32.0	32.0	32.0	0.0
200	33.0	33.0	33.5	33.2	0.3	27.0	27.5	27.0	27.2	0.3
400	25.0	25.0	25.5	25.2	0.3	28.0	28.0	28.0	28.0	0.0
600	34.0	34.0	34.0	34.0	0.0	29.0	28.5	28.5	28.7	0.3
800	34.0	34.0	33.5	33.8	0.3	24.0	24.0	24.0	24.0	0.0
1000	38.0	38.0	38.0	38.0	0.0	36.0	36.0	36.5	36.2	0.3

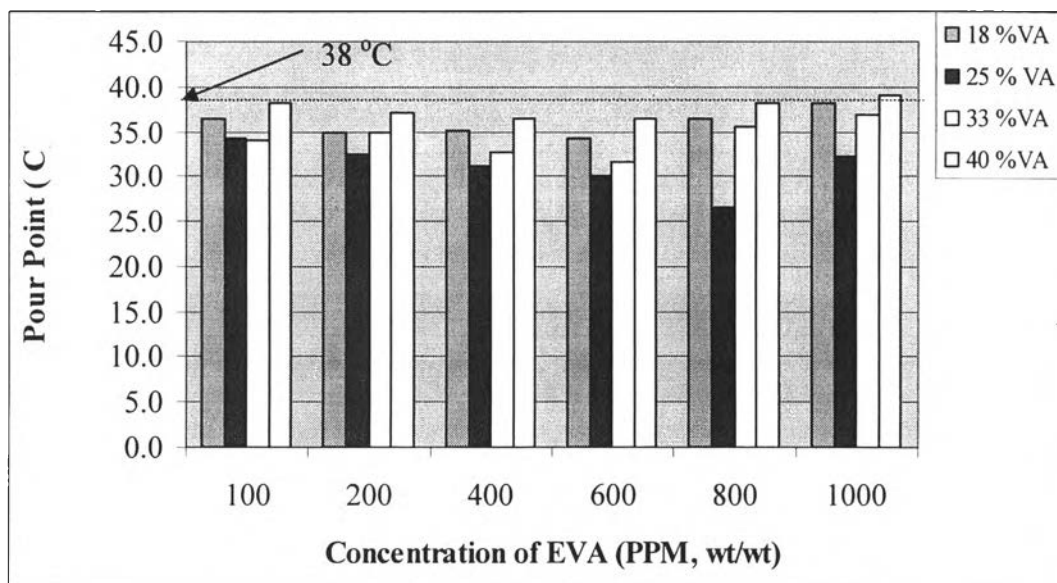


**Figure 4.35** Relationship between pour point of treated Lankrabue crude oil by EVA and concentration of EVA at any percent content of VA.

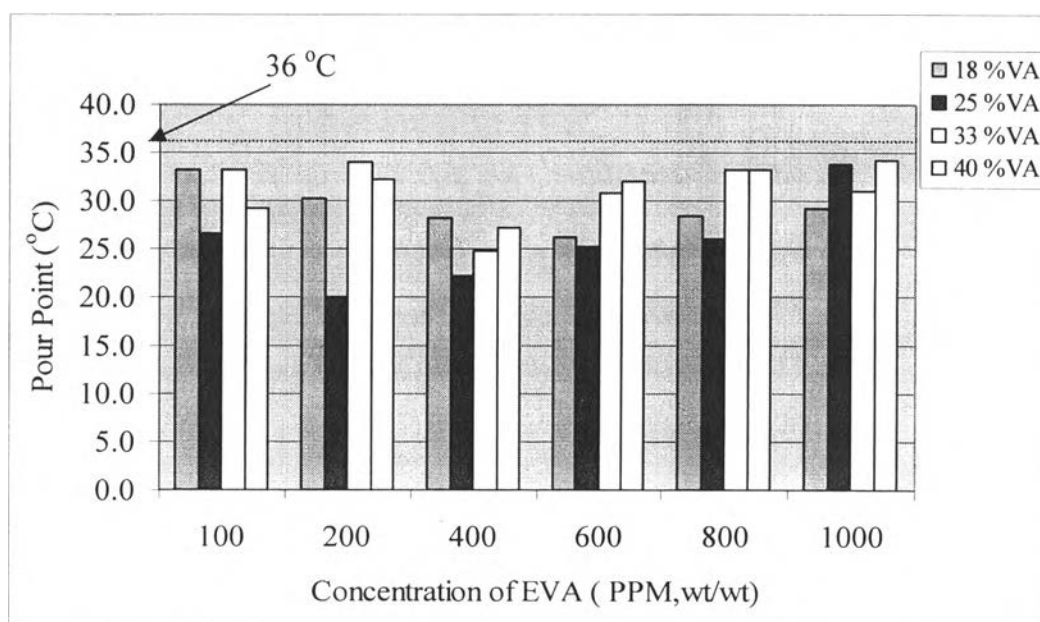


**Figure 4.36** Relationship between pour point of treated U-Thong crude oil by EVA and concentration of EVA at any percent content of VA.

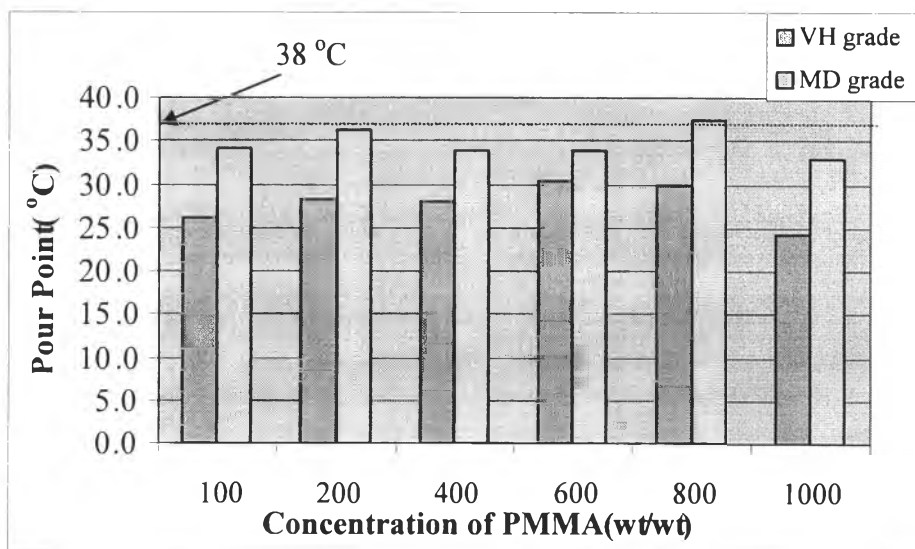


**Figure 4.37** Relationship between pour point of treated Lankrabue crude oil and concentration of two commercial grades, VH and MD, of PMMA as obtained from Diapolyacrylate Co.,Ltd.

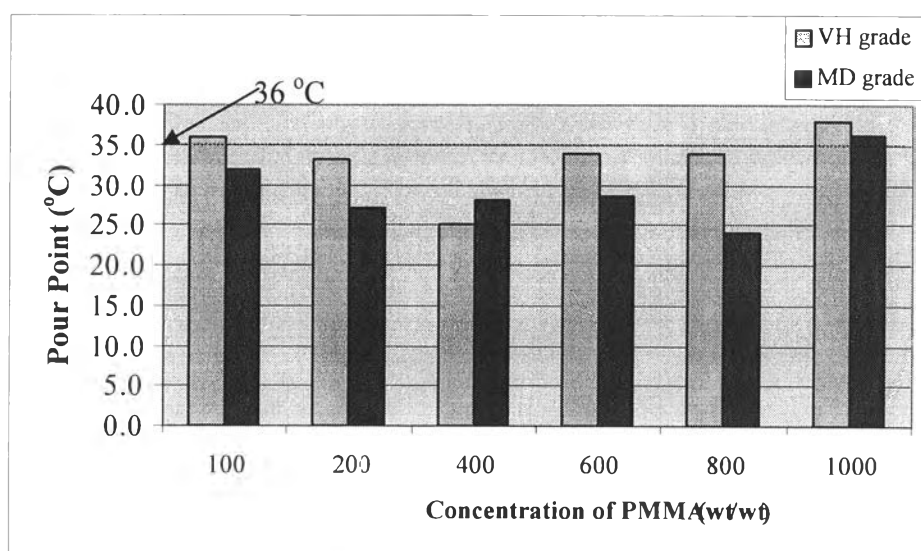


**Figure 4.38** Relationship between pour point of treated Lankrabue crude oil and concentration of two commercial grades, VH and MD, of PMMA as obtained from Diapolyacrylate Co.,Ltd.

The chemicals considered in this work are wax crystal modifiers (wax inhibitors). They have the capacity to enter into wax crystals and alter the growth and surface characteristic of wax crystals. To select a suitable wax modifier, one has to consider the molecular weight or some characteristic chain length of the inhibitor and the molecular weight of the affected wax molecules. It is possible to design wax inhibitors suited for given oils and given operation.

In this work, the EVA was selected. The reasons are;

- 1) It is commonly used in oil industry.
- 2) Its structure is very similar to crude oil in non-polar part i.e., poly (ethylene) although its copolymer, vinyl acetate, is polar but it contributes very little significant to the total polarity of EVA.

- 3) It has been reported (Zhang *et al.*, 2004) that when EVA interacts with the wax crystals, the distance between EVA molecule and wax molecule neighboring to it increases. This significant change will bend wax molecules attached to EVA molecule so it will give more obstacles to the other wax molecules in crude oil to deposit on the wax crystals with steric hindrance effect.

However, the percent content VA should correspond with the major range of hydrocarbons in crude oil. The selected range of percent content of vinyl acetate (VA) was considered by using two factors. The first one is by GC chromatograms of both crude oils which indicated that the major hydrocarbons that cause wax deposition are in the range of carbon atom number, C<sub>14</sub>-C<sub>24</sub>. The second one is by the relationship between percent VA and carbon atom number at each section in EVA copolymer that were separated by carboxylate group as reported by Zhang *et al.* (2004). Therefore, the expected suitable percent content of VA in EVA to reduce the pour point of both crude oils was in the range of 18-40 %.

Moreover, in oil industry, the other wax inhibitor which is sometime used to reduce the pour point of crude oil is poly (methyl methacrylate), PMMA, which has higher polarity than EVA because it consists of ester group, so it is more difficult to dissolve in crude oil. In this work, it was also used to study the influence on pour point of both crude oils and its results were compared with EVA.

From the result, as seen in Tables 4.5, 4.6, 4.7, and 4.8, respectively, the different crude oils were effected differently by different wax inhibitors. Maximum pour point reduction of Lankrabue crude oil was obtained by adding PMMA, and of U-Thong crude oil was obtained by adding EVA.

The suggested mechanisms of wax inhibitors (or wax crystal modifier) by Yun *et al.* (2000) are sequestering mechanism, incorporation-perturbation mechanism, and wax crystal adsorption mechanism.

1) The sequestering mechanism is that the inhibitors make long alkanes in oil less available to nucleate a wax crystal by building into network structure of wax.

2) The incorporation-perturbation mechanism is that inhibitor partition from the oil into amorphous wax, “soft wax” slows down the crystallization of soft wax to form “hard wax”.

3) The wax crystal adsorption mechanism is that adsorption of inhibitors on initial wax nuclei or growing wax crystals inhibits further wax growth.

The overall effect is that the inhibitors will prevent formation of the thermodynamically favorable wax crystal structure until a different crystalline is formed, unaffected by inhibitors, becomes thermodynamically more favorable. However, it is uncertain that which mechanism a wax inhibitor will function therefore it is possible that PMMA and EVA may use one or combination of those mechanisms that may differ. Detailed study and more sophisticated analysed are needed.